A new elastoviscoplastic model based on the Herschel-Bulkley viscoplastic model

Pierre Saramito

December 1, 2008

Abstract – The aim of this paper is to introduce a new three-dimensional elastoviscoplastic model that combines both the Oldroyd viscoelastic model and the Herschel-Bulkley viscoplastic model with a power-law index $n > 0$. The present model is derived to satisfy the second law of thermodynamics. Various fluids of practical interest, such as liquid foams, droplet emulsions or blood, present such elastoviscoplastic behavior: at low stress, the material behaves as a viscoelastic solid, whereas at stresses above a yield stress, the material behaves as a fluid. When $n = 1$, a recently introduced elastoviscoplastic model proposed by the author is obtained. When $0 < n < 1$, then the plasticity criteria becomes smooth, the elongational viscosity is always well defined and the shear viscosity shows a shear thinning behavior. This is a major improvement to the previous elastoviscoplastic model. Finally, when $n > 1$, the material exhibits the unusual shear thickening behavior.
Keywords – non-Newtonian fluid; viscoelasticity; viscoplasticity; constitutive equation.

1 Introduction

In 1926, Herschel and Bulkley [11] proposed a power law variant of the viscoplastic Bingham model [2] :

$$\left\{\begin{array}{ll} |\tau| \leq \tau_0 & \text{when } \dot\varepsilon = 0 \\ \tau = k|\dot\varepsilon|^{n-1}\dot\varepsilon + \tau_0 \dfrac{\dot\varepsilon}{|\dot\varepsilon|} & \text{otherwise} \end{array}\right. \iff \max\left(0,\ \frac{|\tau|-\tau_0}{k|\tau|^n}\right)^{\frac{1}{n}} \tau = \dot\varepsilon$$

where τ is the stress, $\dot\varepsilon$ the rate of deformation, $k > 0$ the consistency parameter and $\tau_0 > 0$ the yield stress. Note that $k|\dot\varepsilon|^{n-1}$ has the dimension of a viscosity. Here, $n > 0$ is the power index. When $n = 1$ the model reduces to the Bingham model. The shear thinning behavior is associated with $0 < n < 1$ and the unusual shear thickening behavior to $n > 1$. In [26], by introducting viscoelasticity into a viscoplastic model, a three-dimensional combination of the viscoelastic Oldroyd and viscoplastic Bingham model has been derived, and has been studied in the context of liquid foam in [5]. The aim of this paper is to explore the elastoviscoplastic extension of the Herschel and Bulkley model, that is written in one-dimensional form:

$$\frac{1}{\mu}\dot\tau + \max\left(0,\ \frac{|\tau|-\tau_0}{k|\tau|^n}\right)^{\frac{1}{n}} \tau = \dot\varepsilon \tag{1}$$

where $\mu > 0$ is the elasticity parameter and $\sigma = \tau + \eta\dot\varepsilon$ is the total stress, where $\eta > 0$ is a viscosity, often called the solvent viscosity in the context of polymer melts. When $n = 1$ and $\tau_0 = 0$ we obtain a one-dimensional version of the Oldroyd viscoelastic model [19]. The new model is motivated by the existence of

materials that exhibit viscoelastic solid-like behavior at low stress and power-index shear thinning fluid-like behavior at high stress. Various authors have fitted their rheological data to the Herschel-Bulkley model with $0 < n < 1$ e.g. [12, 14, 15, 16, 22, 29], in a variety of elastoviscoplastic applications that include concentrated Carbopol micro-gel dispersions, liquid foams and biological flows containing cells. Notice also that Laun (see [17, p. 265] and related references) points out the unusual shear thickening behavior ($n > 1$ case) for suspensions of solid particles.

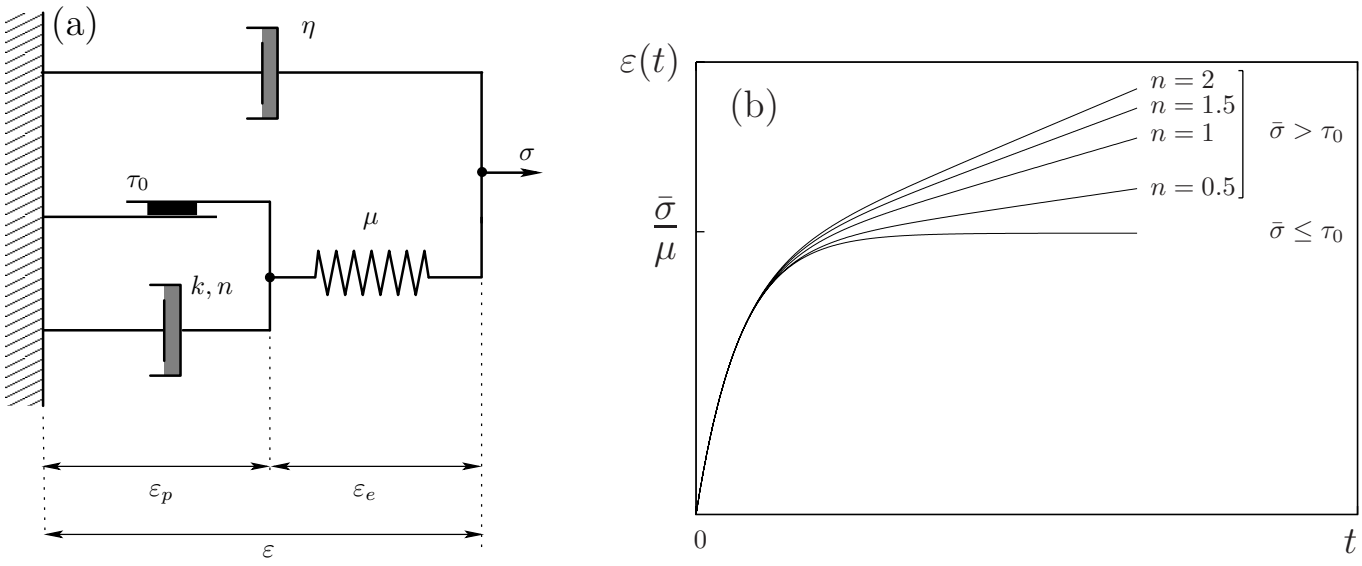

Figure 1: Creeping test for the present model.

The mechanical model is represented in Fig. 1a. At stresses below the yield stress, the friction element remains rigid. The level of the elastic strain energy required to break the friction element is determined by the von Mises yielding criterion. Consequently, before yielding, the whole system predicts only recoverable Kelvin-Voigt viscoelastic deformation due to the spring μ and the viscous element η. The elastic behavior $\tau = \mu\varepsilon$ is expressed in (1) in differential form, where τ denotes the elastic stress. Before yielding, the total stress is $\sigma = \mu\varepsilon + \eta\dot{\varepsilon}$. As soon as the strain energy exceeds the level required by the von Mises criterion, the elastic stress in the friction element attains the yield value and the element breaks allowing deformation of all the other elements. After yielding, the deformation of these elements describes a non-linear viscoelastic behavior.

The evolution in time of elongation $\varepsilon(t)$ for a fixed imposed traction $\overline{\sigma}$ (creeping) is represented on Fig 1b. When $\overline{\sigma} \leq \tau_0$, the elongation for a fixed imposed traction is bounded in time: the material behaves as a Kelvin-Voigt viscoelastic solid. Otherwise, $\overline{\sigma} > \tau_0$, the elongation is unbounded in time: the material behaves as a viscoelastic fluid. A number of other closely related models have appeared in the literature and an historical presentation in 2005 is available in [26]. More recently, in 2007, Fusi and Farina [7] proposed a new model that combines an elastic solid before yielding and a Newtonian fluid after yielding. Based on an explicit description of the free surface separating the solid and the fluid parts, this model leads to complex formulations and computations, even for some simple shear flows such as the Poiseuille flow. In 2008, Benito et al. [1] performed a review of the subject and proposed a classification of elastoviscoplastic models. Combining a solid Burger material before yielding and a viscoelastic fluid after yielding, these authors proposed also a variant of the model [26].

The aim of the present article is to build the proposed model for the general three-dimensional case (section 2) and to study it with simple shear and extensional flows (section 3). The impatient reader – and the reader who is unfamiliar with the thermodynamic framework – could jump directly to the end of section 2 where

the complete set of equations (7) governing such a flow is presented, before reading section 3 devoted to applications.

2 The proposed model

2.1 Thermodynamic framework

The state of the system is described by using two independent variables : the total deformation tensor ε and an internal variable, the elastic deformation tensor ε_e. We have $\varepsilon = \varepsilon_e + \varepsilon_p$ where ε_p represents the plastic deformation tensor. Following Halphen and Nguyen [10] (see e.g. [28] or [18, p. 97]) we say that a *generalized standard material* is characterized by the existence of a free energy function $\mathcal{E}$ and a potential of dissipation $\mathcal{D}$, that are both convex functions of their arguments. The proposed model can be written as:

$$\begin{array}{rcl} \mathcal{E}\left(\varepsilon,\, \varepsilon_e\right) & = & \mu \left|\varepsilon_e\right|^2, \\ \mathcal{D}\left(\dot{\varepsilon},\, \dot{\varepsilon}_e\right) & = & \varphi\left(\,\dot{\varepsilon}\,\right) + \varphi_p\left(\dot{\varepsilon} - \dot{\varepsilon}_e\right), \end{array} \tag{2}$$

where $\mu > 0$ is the elasticity parameter and where $|.|$ denotes the matrix norm, defined by a double contraction of indices : $\left|\varepsilon_e\right|^2 = \varepsilon_e : \varepsilon_e$. The functions φ and φ_p are expressed by :

$$\varphi\left(\dot{\varepsilon}\right) = \left\{ \begin{array}{ll} \eta \left|\,\dot{\varepsilon}\,\right|^2 & \text{when } \operatorname{tr}\dot{\varepsilon} = 0, \\ +\infty & \text{otherwise,} \end{array} \right. \quad \text{and} \quad \varphi_p\left(\dot{\varepsilon}_p\right) = \left\{ \begin{array}{ll} \dfrac{2k}{n+1}\left|\dot{\varepsilon}_p\right|^{n+1} + \tau_0\left|\dot{\varepsilon}_p\right| & \text{when } \operatorname{tr}\dot{\varepsilon}_p = 0, \\ +\infty & \text{otherwise.} \end{array} \right. \tag{3}$$

When $n = 1$, the model coincides with the elastoviscoplastic model introduced in [26] that combines the Bingham and the Oldroyd models. The φ function expresses the incompressible viscous behavior and is associated with the viscosity $\eta \geq 0$ while the φ_p function expresses the viscoplastic behavior by using a power law index $n > 0$ and a consistency parameter $k > 0$, acting on continuous modification of the network links, and also a yield stress value $\tau_0 \geq 0$. When the elastic stress becomes higher than this value, some topological modifications appear in the network of contacts. This model satisfies the second law of thermodynamics: in the framework of *generalized standard materials*, see [10, 28, 18]. This property is a direct consequence of the convexity of both $\mathcal{E}$ and $\mathcal{D}$.

2.2 The general constitutive law

Let Ω be a bounded domain of $\mathbb{R}^N$, where $N = 1, 2, 3$. Since both φ and φ_p are non-linear and non-differentiable, the following manipulations involve subdifferential calculus from convex analysis. The material constitutive laws can be written as:

$$\sigma \in \frac{\partial \mathcal{E}}{\partial \varepsilon} + \frac{\partial \mathcal{D}}{\partial \dot{\varepsilon}} \qquad \text{and} \qquad 0 \in \frac{\partial \mathcal{E}}{\partial \varepsilon_e} + \frac{\partial \mathcal{D}}{\partial \dot{\varepsilon}_e}, \tag{4}$$

where σ is the total Cauchy stress tensor. Using definition (2) of $\mathcal{E}$ and $\mathcal{D}$, we get:

$$\sigma \in \partial\varphi\left(\dot{\varepsilon}\right) + \partial\varphi_p\left(\dot{\varepsilon} - \dot{\varepsilon}_e\right) \qquad \text{and} \qquad 0 \in 2\mu\varepsilon_e - \partial\varphi_p\left(\dot{\varepsilon} - \dot{\varepsilon}_e\right). \tag{5}$$

The combination of the two previous relations leads to $\sigma - 2\mu\varepsilon_e \in \partial\varphi(\dot{\varepsilon})$. Then, by using equation (11) from appendix A, and by introducing the pressure field p, we get the following expression of the total Cauchy stress tensor: $\sigma = -p.I + 2\eta\dot{\varepsilon} + 2\mu\varepsilon_e$ when $\operatorname{tr}(\dot{\varepsilon}) = 0$. Then, the second relation in (5) is equivalent

to $\dot{\varepsilon} - \dot{\varepsilon}_e \in \partial\varphi_p^*(2\mu\varepsilon_e)$ where φ_p^* is the dual of φ_p. Let us introduce the elastic stress tensor $\tau = 2\mu\varepsilon_e$. Equation (10) in appendix A gives the expression for $\partial\varphi^*$, which yields:

$$\frac{1}{2\mu}\dot{\tau} + \max\left(0,\, \frac{|\tau_d| - \tau_0}{2k\,|\tau_d|^{r-1}}\right)^{\frac{1}{n}} \tau \;=\; \dot{\varepsilon} \tag{6}$$

where $\tau_d = \tau - \frac{1}{N}\operatorname{tr}(\tau)\, I$ denotes the deviatoric part of τ.

2.3 The system of equations

Since the material is considered in large deformations, we choose to use the Eulerian mathematical framework, more suitable for fluid flow computations. We assume that $\dot{\varepsilon} = D(\mathbf{v}) = \left(\nabla\mathbf{v} + \nabla\mathbf{v}^T\right)/2$ is the rate of deformation, while the material derivative $\dot{\tau}$ of tensor τ in the Eulerian framework is expressed by the Gordon-Schowalter derivative [8] : $\overset{\square}{\tau} = \frac{\partial\tau}{\partial t} + \mathbf{v}.\nabla\tau + \tau W(\mathbf{v}) - W(\mathbf{v})\tau - a\,(\tau D(\mathbf{v}) + D(\mathbf{v})\tau)$ where $W(\mathbf{v}) = \left(\nabla\mathbf{v} - \nabla\mathbf{v}^T\right)/2$ is the vorticity tensor. The material parameter $a \in [-1, 1]$ is associated with the Gordon-Schowalter's derivative. When $a = 0$ we obtain the Jaumann derivative of tensors, while $a = 1$ and $a = -1$ are associated with the upper and the lower convected derivatives, respectively.

The elastoviscoplastic fluid is then described by a set of three equations associated with three unknowns $(\tau, \mathbf{v}, p)$: the differential equation (6) is completed with the conservation of momentum and mass:

$$\left\{\begin{array}{rcl} \dfrac{1}{2\mu}\overset{\square}{\tau} + \max\left(0,\, \dfrac{|\tau_d| - \tau_0}{2k\,|\tau_d|^{n}}\right)^{\frac{1}{n}} \tau \;-\; D(\mathbf{v}) &=& 0, \\ \rho\left(\dfrac{\partial\mathbf{v}}{\partial t} + \mathbf{v}.\nabla\mathbf{v}\right) - \mathbf{div}\;(-pI + 2\eta D(\mathbf{v}) + \tau) &=& \mathbf{f}, \\ \operatorname{div}\mathbf{v} &=& 0, \end{array}\right.$$

where ρ denotes the constant density and $\mathbf{f}$ a known external force, such as the gravity. These equations are completed by some suitable initial and boundary conditions in order to close the system. For instance the initial conditions $\tau(t{=}0) = \tau_0$ and $\mathbf{v}(t{=}0) = \mathbf{v}_0$ and the boundary condition $\mathbf{v} = 0$ on the boundary $\partial\Omega$ are convenient. The total Cauchy stress tensor can be written as:

$$\sigma = -pI + 2\eta D(\mathbf{v}) + \tau.$$

Note that the incompressibility condition has been enforced by the definition of φ in (3): $\dot{\varepsilon}$ is deviatoric and, since $\dot{\varepsilon} = D(\mathbf{v})$, we get the incompressibility condition $\operatorname{div}\mathbf{v} = \operatorname{tr}\dot{\varepsilon} = 0$. Conversely, the definition of φ_p in (3) enforce that $\dot{\varepsilon}_p$ is deviatoric. While $\dot{\varepsilon}_e = \dot{\varepsilon} - \dot{\varepsilon}_p$ and the elastic stress tensor $\tau = 2\mu\dot{\varepsilon}_e$ are expected to be deviatoric, the replacement of $\dot{\tau}$ by the Gordon-Schowalter tensor derivative $\overset{\square}{\tau}$ do not preserve this property. Instead, the non-deviatoric component of the elastic stress, that acts as an extra pressure component, decays over the elastic timescale.

2.4 Dimensionless formulation

Let U, L be some characteristic velocity and length of the flow, respectively. Let us introduce $\eta_p = k(L/U)^{1-n}$, that has the dimension of a viscosity, and $\eta_0 = \eta + \eta_p$ that denotes the total viscosity. Let $\lambda = \eta_p/\mu$ that has the dimension of a time. Let $T = L/U$ and $\Sigma = (\eta + \eta_p)U/L$ be some characteristic time and stress, respectively. We introduce the following classical dimensionless numbers:

$$We = \frac{\lambda U}{L}, \quad Bi = \frac{\tau_0 L}{\eta_0 U} \;\text{ and }\; Re = \frac{\rho U L}{\eta_0}$$

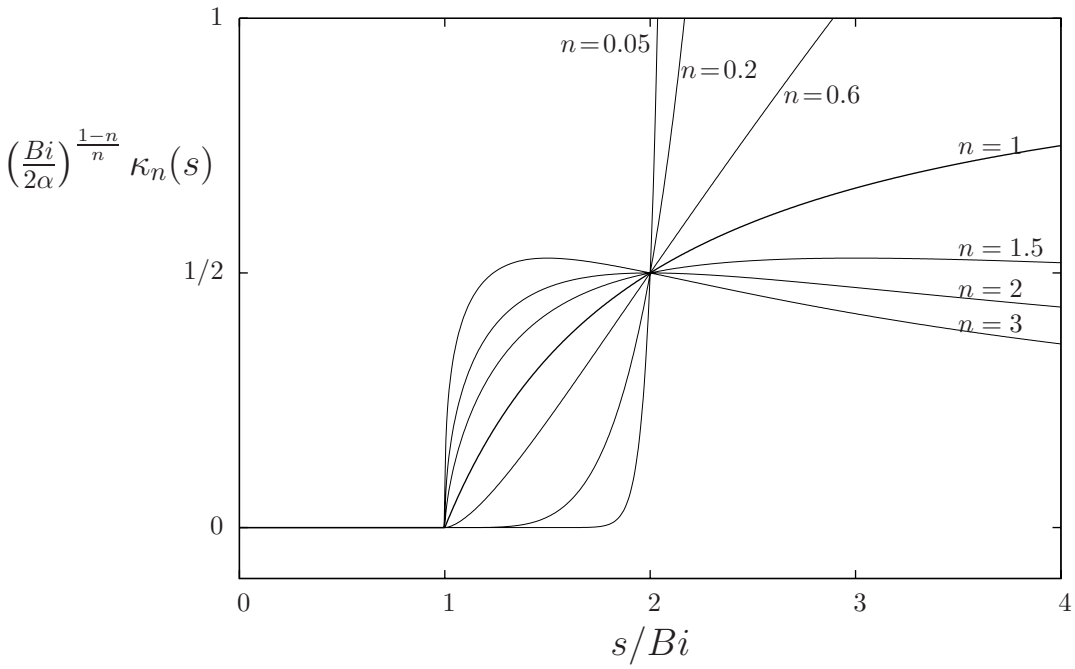

Figure 2: The Herschel-Bulkley plasticity criteria function κ_n for various n values.

which are the Weissenberg, Bingham and Reynolds numbers, respectively. The Weissenberg number is the ratio of the material time scale λ by the experiment characteristic timescale L/U while the Bingham number is the ratio of the yield stress σ_0 to the characteristic viscous stress. We use also the retardation parameter $\alpha = \eta_p/\eta_0 \in]0, 1]$. The problem reduces to that of finding dimensionless fields, also denoted by $(\tau, \mathbf{v}, p)$ such that:

$$\left\{ \begin{array}{rcl} We\, \overset{\square}{\tau} + \kappa_n(|\tau_d|)\,\tau - 2\alpha D(\mathbf{v}) & = & 0, \\ Re\left(\dfrac{\partial \mathbf{v}}{\partial t} + \mathbf{v}.\nabla \mathbf{v}\right) - \mathbf{div}\,(-pI + 2(1-\alpha)D(\mathbf{v}) + \tau) & = & \mathbf{f}, \\ \operatorname{div} \mathbf{v} & = & 0, \end{array} \right. \tag{7}$$

where κ_n denotes the plasticity criteria function :

$$\kappa_n(s) = \max\left(0,\, \frac{s - Bi}{(2\alpha)^{1-n}\; s^n}\right)^{\frac{1}{n}}, \quad \forall s \geq 0 \tag{8}$$

and $\mathbf{f}$ denotes some known dimensionless vector field. These equations are completed by the initial and boundary conditions. Notice that when $We = 0$ and $\alpha = 1$ the model reduces to the viscoplastic Herschel-Bulkley model and when $Bi = 0$ and $n = 1$ it reduces to the usual viscoelastic Oldroyd model [20, 25]. When both $We = Bi = 0$ and $n = 1$ the fluid is Newtonian and the set of equations reduces to the classical Navier-Stokes equations. Conversely, when both $We \neq 0$ and $Bi \neq 0$ the fluid is elastoviscoplastic.

Fig. 2 plots a scaled version of the κ_n function for various values of n. Observe the $\kappa_n(s)$ behavior at $s = Bi$. The function is continuous and its left derivative is zero while its right derivative is also zero when $n < 1$, it is $1/Bi$ when $n = 1$ and $+\infty$ when $n > 1$. As a consequence, the function is smooth, i.e. its derivative is continuous, at $s = Bi$ if and only if $0 < n < 1$. Observe also that, when $0 < n < 1$, then κ_n is unbounded. Conversely, when $n \geq 1$, then κ_n is bounded in $\mathbb{R}^+$ by a value denoted by κ_n^* that depend upon n, Bi and

α. More precisely, the derivative of κ_n is:

$$\kappa_n'(s) = \frac{(s-Bi)^{\frac{1-n}{n}}}{(2\alpha)^{\frac{1-r}{n}} s^2} \left(Bi + \left(\frac{1-n}{n} \right) s \right), \quad \forall s > Bi$$

and then, for $n \geq 1$, κ_n reaches its maximum κ_n^* at $s^* = \left(\frac{n}{n-1} \right) Bi$ and

$$\kappa_n^* = \begin{cases} 1 & \text{when } n = 1 \\ \left(\frac{2\alpha}{Bi} \right)^{\frac{n-1}{n}} \frac{(n-1)^{\frac{n-1}{n}}}{n} & \text{when } n > 1 \end{cases}$$

These basic properties of κ_n are essential for studying the model with practical examples. This is the subject of the following section.

3 Examples

3.1 Uniaxial elongation

The fluid is at rest at $t = 0$ and a constant elongational rate $\dot{\varepsilon}_0$ is applied: the Weissenberg number is $We = \lambda \dot{\varepsilon}_0$ and the Bingham number $Bi = \tau_0/(\eta_0 \dot{\varepsilon}_0)$. All quantities presented in this paragraph are dimensionless.

The flow is three-dimensional and the dimensionless velocity gradient is $\nabla \mathbf{v} = \mathrm{diag}(1, -1/2, -1/2)$. The problem reduces to find τ_{11}, τ_{22} and τ_{33} such that

$$\begin{cases} We \dfrac{\mathrm{d}\tau_{11}}{\mathrm{d}t} & + & (\kappa_n(|\tau_d|) - 2aWe)\tau_{11} & = & 2\alpha, \\ We \dfrac{\mathrm{d}\tau_{jj}}{\mathrm{d}t} & + & (\kappa_n(|\tau_d|) + aWe)\tau_{jj} & = & -\alpha, \quad j = 2, 3 \end{cases}$$

with the initial condition $\tau(t{=}0) = 0$. Since $\tau_{33} = \tau_{22}$ we have: $|\tau_d| = (2/3)^{\frac{1}{2}} |\tau_{11} - \tau_{22}|$. Since $\tau(0) = 0$ and $\tau(t)$ is continuous, there exists $t_0 > 0$ such that when $t \in [0, t_0]$ we have $|\tau_d| \leq Bi$ and thus $\kappa_n = 0$: this is the linear flow regime. The eigenvalues of the system are $2a$ and $-a$. For $t > t_0$, the case $\kappa_n(|\tau_d|) > 0$ occurs. When $n \geq 1$, since κ_n is bounded by κ_n^*, when $aWe > \kappa_n^*/2$ the elastic stress is unbounded. Fig. 3a that plots the *elongational viscosity* η_e^+ normalized by $3\eta_0$ (see e.g. [3, p. 132]). The ratio $3\eta_0$ is the elongational viscosity for a Newtonian fluid. Note that for our dimensionless system we have $\eta_e^+/(3\eta_0) = (\tau_{11} - \tau_{22})/3$. Conversely, when $0 < n < 1$, since κ_n is strictly increasing and unbounded in $\mathbb{R}^+$, the factor $\kappa_n(|\tau_d|) - 2aWe$ remains positive for large $|\tau_d|$. Then the system is amortized and the solution always remains bounded. This feature when $0 < n < 1$ is an important improvement to the case $n = 1$ that was previously considered in [26].

This drawback for $n \leq 1$ is still true for the Oldroyd viscoelastic model, i.e. when $n = 1$ and $Bi = 0$. In the context of viscoelastic models, some alternate constitutive equations that extend the Oldroyd model have been proposed, such as the Phan-Thien and Tanner model [21, 25] and the FENE-P model [4].

The stationary problem reduces to find τ_{11} and τ_{22} such that

$$\begin{cases} (\kappa_n(|\tau_d|) - 2aWe)\tau_{11} & = & 2\alpha \\ (\kappa_n(|\tau_d|) + aWe)\tau_{22} & = & -\alpha \end{cases}$$

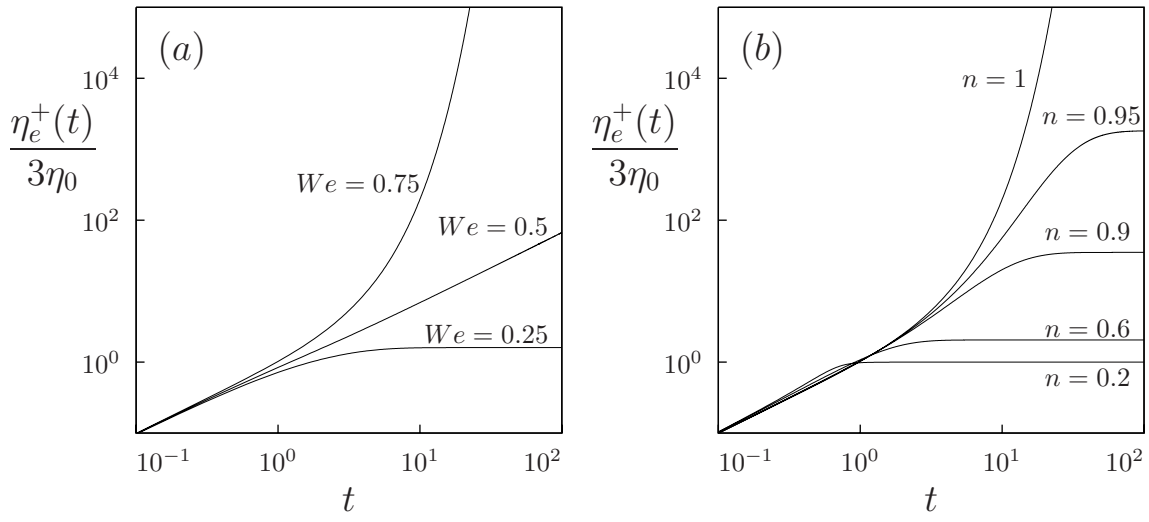

Figure 3: Normalized elongational viscosity $\eta_e^+(t)/(3\eta_0)$ for uniaxial elongation when $Bi=1$, $a=1$ and $\alpha=1$: (a) influence of We for $r=2$; (b) influence of n for $We=0.75$.

When $a = 0$ the stationary solution is independent of We and $\psi = (\tau_{11} - \tau_{22})/2$ satisfies: $\kappa_n(|\tau_d|)\psi = 3\alpha/2$. Then $\psi \geq 0$ and $|\tau_d| = \sqrt{8/3}\ \psi$. The previous equation leads to the following explicit expression of the steady elongational viscosity η_e:

$$\frac{\eta_e}{3\eta_0} = 1 - \alpha + (2/3)\psi = 1 - \alpha + (2/3)^{\frac{1-n}{2}}\alpha \ + \ (2/3)^{\frac{1}{2}}Bi$$

Note that when $a = 0$, $n = 1$ and $Bi = 0$, we obtain the classical result $\eta_e = 3\eta_0$ i.e. the elongational viscosity in the Newtonian case is three times the total viscosity.

Fig. 4 plots the normalized steady elongational viscosity when $a = 1$. The computation is no longer explicit for $a \neq 0$, and requires numerical solution. We observe that it depends upon We, while it was independent of We when $a = 0$. Moreover, when $n \geq 1$, there exists a critical value of We upon which the elongational viscosity is no longer defined. Conversely, when $0 < n < 1$, the elongational viscosity is defined for any We and is an increasing function of We.

3.2 Simple shear flow

The fluid is at rest at $t = 0$ and a constant shear rate $\dot{\gamma}_0$ is applied: the Weissenberg number is $We = \lambda\dot{\gamma}_0$ and the Bingham number $Bi = \tau_0/(\eta_0\dot{\gamma}_0)$.

The flow is two-dimensional and the dimensionless velocity gradient is constant: $\nabla\mathbf{v} = ([0,1];[0,0])$. The problem reduces to finding τ_{11}, τ_{22} and τ_{12}, such that, for all $t > 0$:

$$We\frac{\mathrm{d}}{\mathrm{d}t}\begin{pmatrix}\tau_{11}\\ \tau_{22}\\ \tau_{12}\end{pmatrix} + (We\mathcal{A}_a + \kappa_n(|\tau_d|).I)\begin{pmatrix}\tau_{11}\\ \tau_{22}\\ \tau_{12}\end{pmatrix} = \begin{pmatrix}0\\ 0\\ \alpha\end{pmatrix},$$

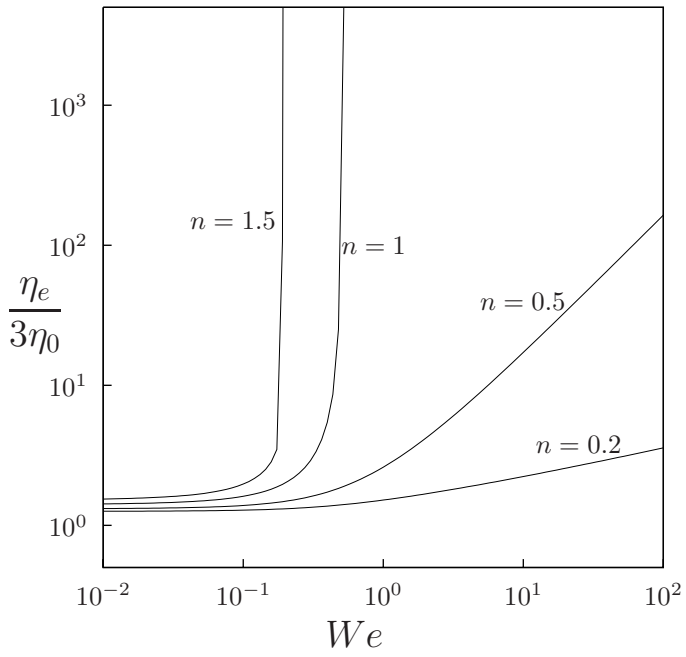

Figure 4: Normalized steady elongational viscosity $\eta_e/(3\eta_0)$ for $a = 1$, $Bi = 1$, $\alpha = 1$.

with the initial condition $\tau(0) = 0$, where

$$\mathcal{A}_a = \begin{pmatrix} 0 & 0 & -(1+a) \\ 0 & 0 & 1-a \\ \dfrac{1-a}{2} & -\dfrac{1+a}{2} & 0 \end{pmatrix}$$

with the initial condition $\tau(0) = 0$ and where $|\tau_d|^2 = (1/2)\left(\tau_{11} - \tau_{22}\right)^2 + 2\tau_{12}^2$. Let $\psi = (\tau_{11} - \tau_{22})/2$ be the dimensionless normal elastic stress difference. Then $\tau_{11} = \dfrac{1+a}{2}\psi$ and $\tau_{22} = -\dfrac{1-a}{2}\psi$. The solution (τ_{12}, ψ) is represented on Fig. 5. Since $\tau(0) = 0$ and $\tau(t)$ is continuous, there exists $t_0 > 0$ such that when $t \in [0, t_0]$ we have $|\tau_d| \leq Bi$ and thus $\kappa_n(|\tau_d|) = 0$: this is the linear flow regime. The eigenvalues of the system are 0 and $\pm i\sqrt{1-a^2}$. At $t = t_0$, $|\tau_d|$ reaches Bi. Then, for $t > t_0$, the non-linear factor $\kappa_n(|\tau_d|) > 0$ occurs: the corresponding term reduces the growth of the solution, which now remains bounded for any $n > 0$.

When $a = 1$ (see Fig. 5, where $\tau_{22} = 0$) the solution tends to a constant value as $t \to \infty$ for any $Bi \geq 0$. Observe on Fig. 5a that τ_{12} presents an overshoot that is more pronounced for small values of n. Conversely, the steady value of $\tau_{11} - \tau_{22}$ is monotonically increasing for any values of n (Fig. 5b). The experimental evidence of non-vanishing first normal stress difference in shear flows can be found in [13] for a liquid foam in a Taylor-Couette geometry. Classical viscoplastic models such as the usual Bingham and Herschel-Bulkley models do not predict first normal stress difference in shear flows: this feature is due to viscoelasticity. Since the present model combines both viscoplasticity and viscoelasticity, it is able to predict yield stress behavior together with first normal stress difference in shear flows. In [5], the numerical prediction with the special case $n = 1$ of the present model has been compared for the Taylor-Couette geometry with experimental data from [13]. We show in Fig. 6 the steady shear viscosity η_s/η_0 (see e.g. [3, p. 104]). as a function of We. Notice that the dimensionless steady shear viscosity η_s/η_0 coincides with the dimensionless steady total shear stress $\sigma_{12} = 1 - \alpha + \tau_{12}$. The material presents a shear thinning character when $0 < n < 1$ and a

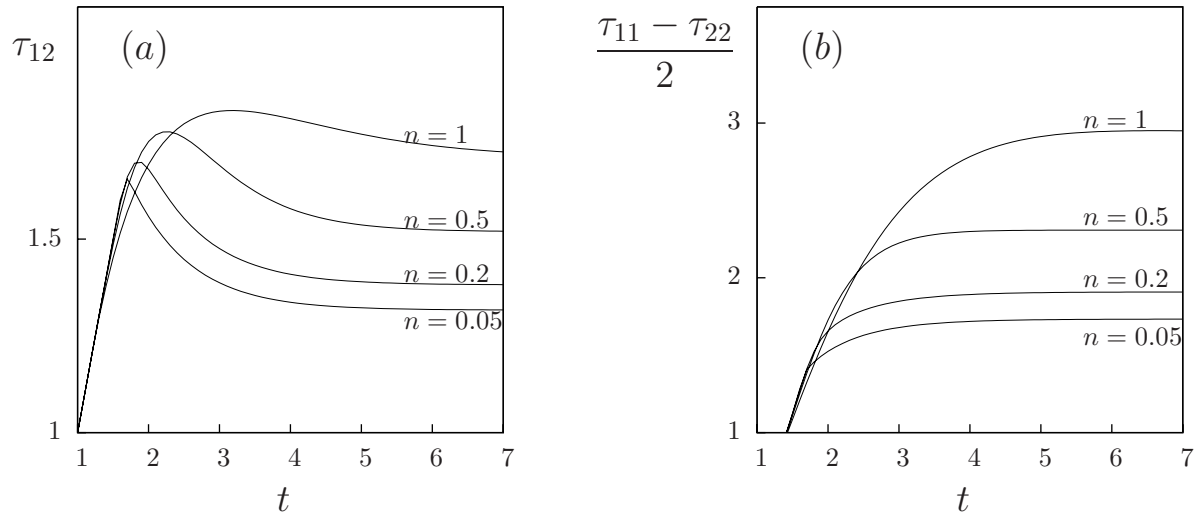

Figure 5: Simple shear flow for $a = 1$, $We = 1$, $Bi = 1$ and $\alpha = 1$: (a) τ_{12}; (b) $(\tau_{11} - \tau_{22})/2$.

shear thickening character when $n > 1$. This feature is a second major improvement to the case $n = 1$ that was previously considered in [26]. For $0 < n < 1$, the shear viscosity decreases monotonically when $\alpha = 1$ (Fig. 6a), and tends to $1 - \alpha$ when $\alpha < 1$, due to the additional viscous contribution to the total shear stress σ_{12}. The shear viscosity tends also to a plateau when $n = 1$ (Fig. 6b) and increases monotonically when $n > 1$ (Fig. 6c). The value of Bi controls the viscosity plateau at small values of We while it has less influence on the viscosity for large values of We. Note that this power-law behavior introduced here together with the Herschel-Bulkley viscoplastic model has been already introduced in the context of generalized Newtonian fluids by Carreau and Yasuda (see e.g. [4, p.171]) in order to be in agreement with shear rheology data.

When $a = 0$ and Bi is small enough (see Fig. 7a, where $\tau_{22} = -\tau_{11}$), the solution tends also to a steady value with decaying oscillations. These oscillations are due to presence of complex eigenvalues in the system. When $a = 0$ and Bi becomes larger, oscillations no longer decay and instabilities appear, while the solution remains bounded (Fig. 7b). The Lissajou plot on Fig. 8 shows the asymptotical orbit of the solution for various values of n. The orbit tangents the von Mises circle associated with $|\tau_d| = Bi$ (dotted lines). When the trajectory enters in the von Mises circle, the trajectory is exactly a circle, since the equations are linear when $\kappa_n(|\tau_d|) = 0$, while when its goes outside the circle, it decays, since the equations are non-linear. and $\kappa_n(|\tau_d|) > 0$. The asymptotical orbit is then completely included in the von Mises circle. We observe that the orbit in the Lissajou plot satisfies :

$$\tau_{12} = R_0 \sin(\omega t + \varphi) \quad \text{and} \quad \psi = \frac{\tau_{11} - \tau_{22}}{2} = 1 + R_0 \cos(\omega t + \varphi)$$

where R_0 is the radius of the orbit and φ is the phase shift that depends upon the initial value. The von Mises criteria for the asymptotical orbit is $\max_t |\tau_d(t)| = Bi$ i.e.:

$$\max_t \left(1 + R_0 \cos(\omega t)\right)^2 + \left(R_0 \sin(\omega t)\right)^2 = Bi^2/2$$

and thus $R_0 = Bi/\sqrt{2} - 1$. Finally, the asymptotical orbit is a circle of radius R_0 and center $(\tau_{12}, \psi) = (0, 1)$ on the Lissajou plane. The power-law parameter n does not change the orbit. It changes the speed of decay, as shown in Fig. 8. Finally, the critical Bingham number at which oscillations no longer decay is $Bi_c = \sqrt{2}$. The shear viscosity η_s is no longer defined when $a = 0$ and We becomes large, since the solution for simple

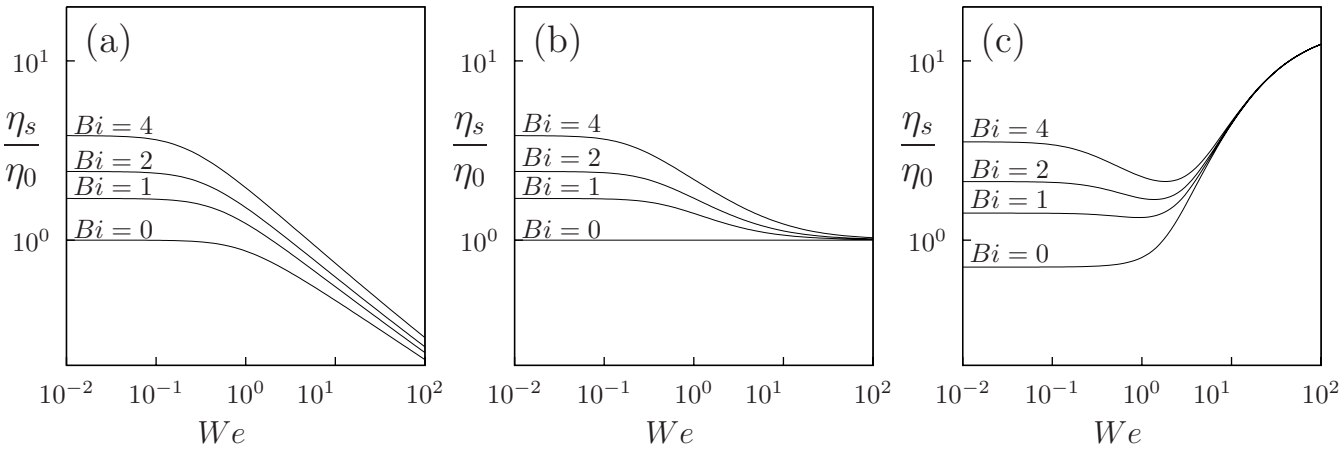

Figure 6: Steady shear viscosity for $a = 1$, $\alpha = 1$ and (a) $n = 0.5$; (b) $n = 1$; (c) $n = 1.5$.

shear flow is no longer stationary and oscillates. The stability of the solution depends upon the values of the dimensionless parameters. This conditional stability is common in the context of viscoelastic models ($Bi = 0$): see e.g. [9] for Poiseuille flow and [27] for Couette-Taylor flows.

4 Conclusion

A new model for elastoviscoplastic fluid flows that is objective and satisfies the second law of thermodynamics is proposed in (7). It extends the previous elastoviscoplatic model introduced in [26] by introducing a power law index $n > 0$. As a major improvement, when $0 < n < 1$ this model presents finite extensional properties and a shear thinning behavior. In [5], the numerical prediction with the present model and in the case when $n = 1$ has been compared for Taylor-Couette geometry with experimental data from [13]. Future work will extends quantitative comparisons between experimental measurements and numerical predictions to the case when $0 < n < 1$. As many elastoviscoplatic materials have been found to exhibit shear thinning behavior, this model is a good candidate for numerical simulation of such materials in complex multi-dimensional geometries (see e.g. [6, 23, 24]).

A Technical details

A.1. The φ_p function – The subgradient $\partial\varphi_p$, as introduced in (3), is defined for any tensor D by:

$$\begin{aligned} \partial\varphi_p(D) &= \{\tau,\ \tau : (H - D) \ \leq\ \varphi_p(H) - \varphi_p(D),\ \forall H\} \\ &= \{\tau,\ j_p(D) \ \leq\ j_p(H),\ \forall H \text{ with } \mathrm{tr}(H) = 0 \text{ and } \mathrm{tr}(D) = 0\}, \end{aligned}$$

with the notation $j_p(H) = \frac{2k}{n+1}|H|^{n+1} + \tau_0|H| - \tau : H$. When the minimizer D of j_p over the set $\{D, \mathrm{tr}\, D = 0\}$ is non vanishing, it satisfies, from the theory of Lagrange multipliers:

$$\nabla j_p(D) - p.I = 0 \ \text{ and } \ \mathrm{tr}(D) = 0,$$

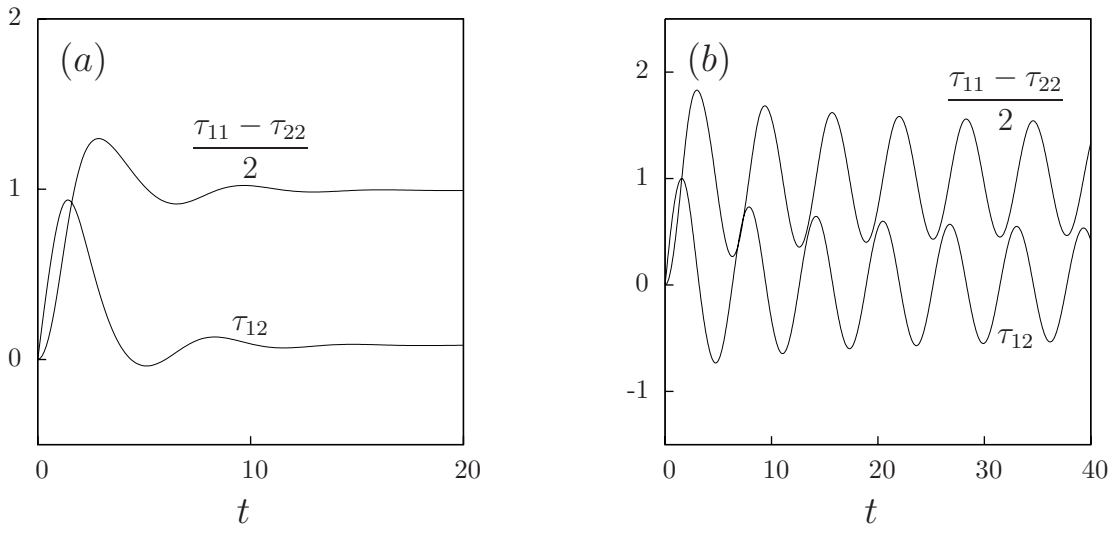

Figure 7: Simple shear flow for $a = 0$, $n = 0.5$, $We = 1$ and $\alpha = 1$: (a) $Bi = 1$; (b) $Bi = 2$.

where p is the Lagrange multiplier. Then $2k|D|^{n-1}D + \tau_0 \dfrac{D}{|D|} - \tau - p.I = 0$ and $\mathrm{tr}(D) = 0$. Thus finally, the subgradient is:

$$\partial\varphi_p(D) = \begin{cases} \{\tau,\ |\tau_d| \le \tau_0\} & \text{when } D = 0, \\ \left\{\tau,\ \tau = -p.I + 2k|D|^{n-1}D + \tau_0 \dfrac{D}{|D|}\right\} & \text{when } D \neq 0 \text{ and } \mathrm{tr}(D) = 0, \\ \emptyset & \text{otherwise,} \end{cases} \tag{9}$$

where τ_d denotes the deviatoric part of τ. The dual φ_p^* of φ_p is then characterized by the Fenchel identity, that is, for any $\tau \in \partial\varphi_p(D)$, by $\varphi_p^*(\tau) = \tau : D - \varphi_p(D)$. Moreover, $\tau \in \partial\varphi_p(D)$ is equivalent to $D \in \partial\varphi_p^*(\tau)$. From $\tau + p.I = (2k|D|^{n-1} + \tau_0/|D|)D$ we get $|\tau_d| = 2k|D|^n + \tau_0$ and thus $|D| = ((|\tau_d| - \tau_0)/(2k))^{1/n}$. Finally:

$$\partial\varphi_p^*(\tau) = \left\{ D,\ D = \max\left(0,\ \frac{|\tau_d| - \tau_0}{2k|\tau_d|^n}\right)^{1/n} \tau_d \right\}, \tag{10}$$

where τ_d denotes the deviatoric part of τ.

A.2. The φ function – The function φ, as introduced in (3), is a particular case of φ_p with $\tau_0 = 0$, $n = 1$ and $k = \eta$. From (9), the subgradient is:

$$\partial\varphi(D) = \begin{cases} \{\tau,\ \tau = -p.I + 2\eta D\} & \text{when } \mathrm{tr}(D) = 0, \\ \emptyset & \text{otherwise.} \end{cases} \tag{11}$$

References

[1] S. Benito, C. H. Bruneau, T. Colin, C. Gay, and F. Molino. An elasto-visco-plastic model for immortal foams or emulsions. *Eur. Phys. J. E*, 25(3):225–251, 2008.

[2] E. C. Bingham. *Fluidity and plasticity.* Mc Graw-Hill, 1922.

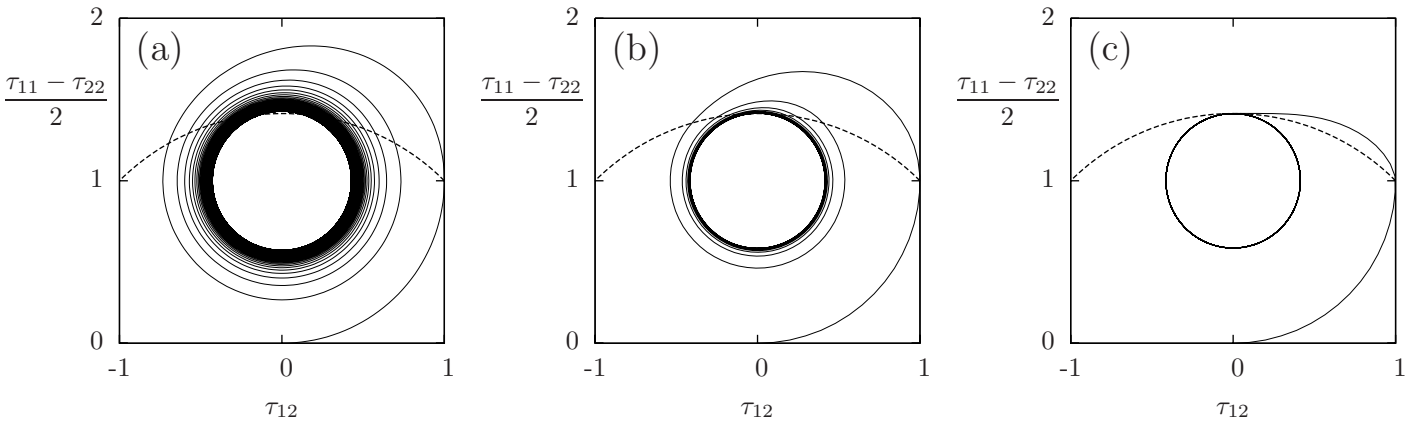

Figure 8: Simple shear flow when $a = 0$, $Bi = 2$ and $We = 1$: flow instabilities and asymptotical orbit when (a) $n = 0.5$; (b) $n = 1$; (c) $n = 2$. The dotted line indicates the von Mises circle.

[3] R. B. Bird, C. F. Curtiss, R. C. Armstrong, and O. Hassager. *Dynamics of polymeric liquids, vol. 1. Fluid mechanics.* J. Wiley, 1987.

[4] R. B. Bird, C. F. Curtiss, R. C. Armstrong, and O. Hassager. *Dynamics of polymeric liquids, vol. 2. Kinetic theory.* J. Wiley, 1987.

[5] I. Cheddadi, P. Saramito, C. Raufaste, P. Marmottant, and F. Graner. Numerical modelling of foam couette flows. *Eur. Phys. J. E*, 27(2):123–133, 2008.

[6] B. Dollet, M. Durth, and F. Graner. Flow of a foam past an elliptical obstacle. *Phys. Rev. E*, 73, 2006.

[7] L. Fusin and A. Farina. Modelling of Bingham-like fluids with deformable core. *Comput. Math. Appl.*, 53(3-4):583–594, 2007.

[8] R. J. Gordon and W. R. Schowalter. Anisotropic fluid theory: a different approach to the dumbbell theory of dilute polymer solutions. *Trans. Soc. Rheol.*, 16:79–97, 1972.

[9] C. Guillopé and J. C. Saut. Global existance and one-dimensional non-linear stability of shearing motions of viscoelastic fluids of Oldroyd type. *Math. Model. Numer. Anal.*, 24:10–11, 1990.

[10] B. Halphen and Q. S. NGuyen. Sur les matériaux standard généralisés. *J. Méca.*, 14:39–63, 1975.

[11] W. H. Herschel and T. Bulkley. Measurement of consistency as applied to rubber-benzene solutions. *Am. Soc. Test Proc.*, 26(2):621–633, 1926.

[12] A. Iordan, A. Duperray, and C. Verdier. Fractal approach to the rheology of concentrated cell suspensions. *Phys. Rev. E*, 77:011911, 2008.

[13] E. Janiaud and F. Graner. Foam in a two-dimensional Couette shear: a local measurement of bubble deformation. *J. Fluid Mech.*, 532:243–267, 2005.

[14] G. Katgert, M. E. Möbius, and M. van Hecke. Rate dependence and role of disorder in linearly sheared two-dimensional foams. *Phys. Rev. Lett.*, 101:058301, 2008.

[15] R. J. Ketz, R. K. Prud'homme, and W. W. Graessly. Rheology of concentrated micro-gel solutions. *Rheol. Acta*, 27:531–539, 1988.

[16] V. J. Langlois, S. Hutzler, and D. Weaire. Rheological properties of the soft disk model of 2D foams. *Phys. Rev. E*, 78:021401, 2008.

[17] R. G. Larson. *The structure and rheology of complex fluids*. Oxford University Press, 1999.

[18] G. Maugin. *The thermomechanics of plasticity and fracture*. Cambridge University Press, 1992.

[19] J. G. Oldroyd. A rational formulation of the equations of plastic flow for a Bingham solid. *Proc. Camb. Philos. Soc.*, 43:100–105, 1947.

[20] J. G. Oldroyd. On the formulation of rheological equations of states. *Proc. Roy. Soc. London*, A 200:523–541, 1950.

[21] N. Phan-Thien and R. I. Tanner. A new constitutive equation derived from network theory. *J. Non-Newtonian Fluid Mech.*, 2:353–365, 1977.

[22] J. M. Piau. Carbopol gels: elastoviscoplastic and slippery glasses made of individual swollen sponges. meso- and macroscopic properties, constitutive equations and scaling laws. *J. Non-Newtonian Fluid Mech.*, 144:1–29, 2007.

[23] N. Roquet, R. Michel, and P. Saramito. Errors estimate for a viscoplastic fluid by using Pk finite elements and adaptive meshes. *C. R. Acad. Sci. Paris, Série I*, 331(7):563–568, 2000.

[24] N. Roquet and P. Saramito. An adaptive finite element method for Bingham fluid flows around a cylinder. *Comput. Appl. Meth. Mech. Engrg.*, 192(31-32):3317–3341, 2003.

[25] P. Saramito. Efficient simulation of nonlinear viscoelastic fluid flows. *J. Non-Newtonian Fluid Mech.*, 60:199–223, 1995.

[26] P. Saramito. A new constitutive equation for elastoviscoplastic fluid flows. *J. Non Newtonian Fluid Mech.*, 145(1):1–14, 2007.

[27] R. Sureshkumar, M. D. Smith, R. C. Armstrong, and R. A. Brown. Linear stability and dynamics of viscoelastic flows using time-dependent numerical simulations. *J. Non-Newtonian Fluid Mech.*, 82(1):57–104, 1999.

[28] P. Le Tallec. *Numerical analysis of viscoelastic problems*. Masson, France, 1990.

[29] D. Weaire, S. Hutzler, V. J. Langlois, and R. J. Clancy. Velocity dependence of shear localisation in a 2D foam. *Philos. Mag. Lett.*, 88:387–396, 2008.